THE JOURNAL OF PHYSICAL CHEMISTRY B

ARTICLE

pubs.acs.org/JPCB

Structural Investigation of Nonionic Fluorinated Micelles by SANS in Relation to Mesoporous Silica Materials

Florentin Michaux,[†] Jean-Luc Blin,[†] José Teixeira,[‡] and Marie José Stébé*[,†]

[†]Equipe Physico-chimie des Colloïdes, UMR SRSMC N° 7565, Université Nancy-1/CNRS Faculté des Sciences, BP 70239, F-54506 Vandoeuvre-les-Nancy cedex, France

[‡]Laboratoire Léon Brillouin (CEA/CNRS), CEA-Saclay, 91191 Gif-sur-Yvette Cedex, France

Supporting Information

ABSTRACT: In an attempt to answer the question if there is dependence between the pore ordering of the mesoporous silica, obtained through the cooperative template mechanism, and the shape of the micellar aggregates of the surfactant solutions, the micellar structures of two nonionic fluorinated surfactant based-systems are studied by SANS. By fitting the experimental spectra with theoretical models, the structural evolution of the molecular aggregates can be described, and some important parameters can be obtained, such as the water and eventually oil penetration into the surfactant film, the aggregation number, the area per polar head of the surfactant, and the surfactant chain conformations. We have shown that for the $C_8F_{17}C_2H_4$-$(OC_2H_4)_9OH$ system, the micelles are prolate spheroids. The increase of the surfactant concentration in water does not change the characteristics of the interfacial film, but the aggregation number raises and the particles become more elongated. By contrast, the experimental curves of $C_7F_{15}C_2H_4(OC_2H_4)_8OH$ cannot be fitted considering a small particle model. However, progressive incorporation of fluorocarbon induces a change of size and shape of the globules, which become smaller and more and more spherical. Regarding the material mesopore ordering, it appears that the micelles that lead to hexagonal mesoporous silica materials are described with a model of quasi-spherical globules. On the contrary, when large micelles are found, only wormhole-like structures are obtained.

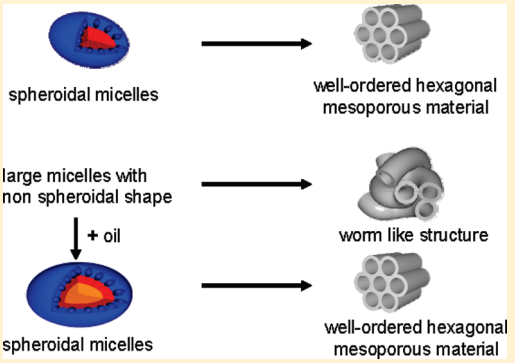

INTRODUCTION

Since the ordered mesoporous materials prepared by Mobil's scientists in 1992,[1] numerous surfactant-based systems have been investigated as structure directing agents.[2] A large series of ionic and nonionic surfactants has been used in the synthesis of ordered mesoporous silica or nonsilica materials. Among the nonionic surfactants, polyoxyethylene alkyl ethers, which are used as emulsifiers, wetting agents, detergents, or solubilizers, have been employed as templates for the preparation of mesoporous compounds.[3] These materials are mainly synthesized from the cooperative template mechanism (CTM),[4] i.e., from micellar solutions. In the initial step, the interactions between silica and isolated micelles drive to the formation of an organic−inorganic hybrid mesophase. Then, the condensation of the inorganic precursor at the external surface of the micelles occurs. The ordered mesophase is obtained after intermicellar condensation. Finally, the hydrothermal treatment at higher temperature completes the assembly of micelles and the polymerization of the silica source. However, some disagreements concerning the first step of the CTM mechanism appear, and numerous investigations have been carried out in order to find a better understanding of how the surfactant micelles and the inorganic precursor could affect the formation of the hybrid mesophase. Thus, many studies are focused on the formation of organized mesoporous materials. In particular, the compounds of the M41S[5,6] and SBA[7−9] families have been investigated by several experimental techniques such as small-angle X-ray[7−9] and neutron scattering[10,11] spectroscopic techniques (NMR, EPR, and IR),[12,13] transmission electron microscopy (TEM),[7] and fluorescence probing techniques.[14] The spectroscopic and TEM experiments are generally carried out ex situ and some modifications of the system can occur during the investigation. By contrast, in situ analyses by SAXS or SANS allow us to observe the transformations of the system in the moment they are taking place. For example, concerning SBA-15, which is prepared by using the triblock copolymer P123, interesting informations have been obtained about the initial stages of its formation by in situ SAXS analysis. As a matter of fact, the scenario proposed by M. Impéror-Clerc et al.[15] and J.S. Pedersen et al.[16] describes the formation of the hexagonal network in three stages. In the first minutes following the addition of the silica source, the micelles of P123 remain spherical. The second step corresponds to the formation of organic−inorganic hybrid micelles, and the

Received: October 13, 2011
Revised: November 29, 2011
Published: December 06, 2011

silicated species are placed in-between the hydrophilic chains of the surfactant. The micelle shape changes from spherical to cylindrical. The beginning of the third stage corresponds to the aggregation of these cylindrical hybrid micelles according to a hexagonal network. Finally, the condensation of the silica continues to form the silica walls of the mesoporous material. Thus, from these results, one can speculate if the pore ordering depends on the micellar phase properties, in particular on the micelle structure.

We already know that the characteristics of the recovered materials, such as the structure and the pore size, are related to the solubilization properties of the surfactant in water. In fact, we have previously shown, with a series of nonionic surfactants, that the pore ordering of the material can be influenced by the temperature at which the silica precursor is added to the micellar solutions.[17] Indeed, this temperature should not be close to the lower consolute curve (lcb), which characterizes the nonionic surfactant-based systems. The lcb delimits the domain of the micellar phase (L_1) to that where two micellar phases exist. It was shown before that micelles grow in size as the temperature rises toward the lcb.[18] Moreover, micellar structure is related to the critical concentration, which corresponds to the minima of the consolute curve.[19] Finally, in the close vicinity of the critical point, critical phenomena exist.[20] Thus, the phenomena associated to the cloud curve likely disturb the CTM, which governs the mesoporous material formation.

However, the formation of the ordered materials is also affected by other properties of the surfactant used for their preparation. According to the concept proposed by Stucky et al.,[21] we have evidenced that for a given set of preparation conditions, the formation of the mesostructured materials is related to the ratio between the volume of the hydrophilic part (V_A) and the hydrophobic part (V_B) of the surfactant. For example, using either polyoxyethylene alkyl ether or polyoxyethylene fluoroalkyl ether surfactants, we have shown that V_A/V_B ratios in the range between 0.95 and 1.78 lead to the formation of well ordered mesostructures.[22] Fluorinated surfactants have been selected, taking into account the equivalence rule between hydrogenated and fluorinated surfactants (i.e., 1 CF_2 is equivalent to 1.7 CH_2).[23] Therefore, the phase behavior in water of these two types of surfactant is similar. Despite the discrepancy in the molar volume, the V_A/V_B range does not depend on the surfactant nature (fluorinated or hydrogenated). Both the position of the cloud point curve and the hydrophilic−hydrophobic molar volume balance are parameters that are related to the structural properties of micelles. In this work, in order to shed some light on the synthesis mechanism of the mesoporous materials, we carried out a structural study by small angle neutron scattering (SANS) of the $C_8F_{17}C_2H_4(OC_2H_4)_9OH$ [$R_8^F(EO)_9$] and $C_7F_{15}C_2H_4(OC_2H_4)_8OH$ [$R_7^F(EO)_8$] surfactant based-systems. Hexagonal molecular sieves have been obtained with $R_8^F(EO)_9$, in a wide range of the surfactant concentration in aqueous solution being 5−25 wt %.[24] By contrast, in the same synthesis conditions,[25] i.e., pH, surfactant/silica molar ratio, hydrothermal temperature, and duration, only wormhole-like structures are recovered with $R_7^F(EO)_8$. For the latter system, the mesopore ordering occurs only when additives are added.[17,25] SANS is a powerful technique to obtain structural information about surfactant systems. In fact, this technique affords the possibility to use the contrast variation method with different water isotopic compositions since the coherent scattering lengths of the proton and deuterium atoms are quite different. Moreover, SANS is appropriated for the study of fluorinated surfactant systems, since the two moieties of the surfactant have very contrasted scattering lengths, the coherent scattering length of the fluorine atom being close to the one of deuterium.

EXPERIMENTAL SECTION

Materials. The used fluorinated surfactants, which were provided by DuPont, have an average chemical composition of $C_8F_{17}C_2H_4(OC_2H_4)_9OH$ and $C_7F_{15}C_2H_4(OC_2H_4)_8OH$. They are, respectively, labeled as $R_8^F(EO)_9$ and $R_7^F(EO)_8$. In both cases, the hydrophilic chain moiety exhibited a Gaussian chain length distribution, and the hydrophobic part is composed of a well-defined mixture of fluorinated tails. They were used as received. Perfluorodecalin ($C_{10}F_{18}$) and D_2O were purchased from Aldrich.

Determination of the Phase Diagram. The binary aqueous systems have been determined between 0 and 80 °C in the whole range of water/surfactant compositions. The samples were prepared by weighting the required amounts of surfactant and water in well-closed glass vials to avoid evaporation. They were left at fixed temperature for some hours in order to reach equilibrium. The phase equilibria were determined by visual observation using crossed polarizers to check the eventual anistropic character of the phases in the samples. Liquid crystal phases were identified by their texture, observed with an optical microscope equipped with cross polarizers, Olympus B50. To find the exact phase boundaries of these liquid crystals domains, additional SAXS measurements were also performed.

Small Angle Neutron Scattering. Measurements were carried out at the Laboratoire Léon Brillouin (Saclay, France) on the PAXE instrument. The wavelength λ was set to 5 Å, and the sample detector distance was 3 m. The wave vectors q are thus in the range from 0.013 to 0.24 $Å^{-1}$. Samples are placed in HELLMA quartz cells of 1 mm thickness. According to semistandard procedures, the measured intensities were corrected for incoherent noise and for quartz cell contribution. The intensity scattered by unit volume was then evaluated on an absolute scale, according to a calibration method based on the transmission of the sample and of H_2O (T_W).[26] As a matter of fact, it was shown that the calibration factor C for the $I_S(\theta)/I_W(\theta)$ ratio (where $I_S(\theta)$ and $I_W(\theta)$ are the measured intensities scattered, respectively, by the sample and the water cell under exactly the same experimental conditions, i.e., the same alignment and the same cell thickness) is given, within a good experimental precision, by

$$C = 4 \log T_W / 8.9(1 - T_W)$$

Such a calibration method takes into account the effective variation with the wavelength of the incoherent intensity scattered by H_2O.

The spectra were further interpreted by using a best fit procedure and making use of the variation contrast method (use of water of various deuteration degree).

The theoretical spectra can be calculated approximately for spherical particles according to the equation

$$I(q) = NF^2(q)S(q) \quad (1)$$

where N is the number density of the particles, F is the form factor, and S is the structure factor, which depends on the total dispersed volume fraction and the interparticle interaction potential. If the particles are not spherical, then eq 1 has to be rewritten as

$$I(q) = \langle F^2(q) \rangle + [S_{ES}(q) - 1]\langle F(q) \rangle^2 \quad (2)$$

Table 1. Minimum Value of Intensity at $q = 0$ (Extinction) if Monodisperse Oil in Water Globules Are Considered: Coherent Scattering Length Density of Water b_w and Corresponding Isotopic Composition of Water

system	b_W (10^{-12} cm)	% D_2O (w/w)
$R_8^F(EO)_9$/water	0.5428	36.7
$R_7^F(EO)_8$/water	05369	36.4
$R_7^F(EO)_8$/water/perfluorodecalin 1%	0.5573	37.4
$R_7^F(EO)_8$/water/perfluorodecalin 3%	0.5962	39.3
$R_7^F(EO)_8$/water/perfluorodecalin 5%	0.6325	41.1
$R_7^F(EO)_8$/water/perfluorodecalin 7%	0.6666	57.2

where the average is over all the orientations of the scatterer, $F(q)$ being the scattered amplitude by the anisotropic particle and $S_{ES}(q)$ the structure factor of the equivalent spherical particle. The term $S(q)$ is calculated for equivalent hard sticky spheres, i.e, for a well potential with a very small width compared with the size of the particles. Typical width values for nonionic micelle or microemulsion are taken as 1 or 2 Å, with a depth of a few kT. The mutilayered spheroidal shape has been chosen to describe the micelles or the microemulsions. Therefore, a numerical integration is performed for the calculation, which takes into account the scattered orientations.

The goal of the fitting procedure is to obtain the good absolute level of the intensities scattered in this whole q range for each experimental curve.[27] The theoretical spectra are calculated from all the data, which are composed of the known data and the parameters that we have to determine. The known data deal with the composition of the system (surfactant, water, and eventually oil), the volume of each molecule or part of it (density and molecular mass), and the molecule length scattering. Moreover, we also know the extended lengths of both the hydrophilic and hydrophobic chains of the surfactant. The unknown parameters are (i) the type of packing of the amphiphiles (or the shape), which is given by the axial ratio of the particle, (ii) the lengths (or conformation) of the hydrophilic (L_A) and hydrophobic (L_B) moieties of the surfactant, (iii) the aggregation number (N), (iv) the penetrations of water inside the hydrophilic part (A) and of oil (if any) inside the hydrophobic part (B) of the aggregates defined, as the number of water (α) and oil (β) molecules per surfactant molecule in the amphiphilic film, respectively, and (v) the area per polar head (σ).

If the system does not contain oil, we assume the existence of two homogeneous concentric zones, leading to a three density system. The addition of oil involves the consideration of a fourth layer, and because of geometrical constraints, all the parameters are not independent anymore. For example, for a given composition and if L_A, L_B, N, and the rate of penetration α are known, the values of β, σ, and the ellipticity are automatically determined. Then, for a given sample, the best fit between the theoretical and experimental curves for several contrasts of water allows the determination of the most probable set of the parameter values.

In this study, 4 contrasts, which correspond to 4 isotopic compositions, have been considered. They were chosen to have no classical diffusion curves. Such features can be obtained by selecting contrasts in the vicinity of the extinction at zero angle. For a given overall composition of the sample and whatever the interparticular interactions, the scattered intensity $I(q = 0)$ is proportional to Z^2, which is the resulting excess scattering length of the aggregates, normalized to one surfactant molecule.[28]

For direct micelles $Z = b_S - (b_W/v_W)v_S$, where b_S and b_W stand for the scattering lengths of surfactant and water, respectively; v_S and v_W correspond to the molar volumes of surfactant and water. Thus, $Z = 0$ for $b_W = (b_S/v_S)v_W$. In the presence of oil, the expression of Z becomes $Z = b_S + (N_O/N_S)b_O - (b_W/v_W)(v_S + (N_O/N_S)v_O)$, with N_O/N_S being the number of oil molecules per surfactant molecule, and b_O and v_O correspond, respectively, to the scattering length and the molar volume of oil.

If $Z = 0$, $b_W = v_W(b_S + (N_O/N_S)b_O)/(v_S + (N_O/N_S)v_O)$. For each investigated system, the scattering length b_W for which $I(0) = 0$ was calculated. This calculation leads to the isotopic compositions of water given in Table 1.

RESULTS

$C_8F_{17}C_2H_4(OC_2H_4)_9OH$ [$R_8^F(EO)_9$] System in Water. The phase diagram has been reported in a previous article.[24] A micellar phase, which is very stable in a large range of temperatures, exists until at least 25% of surfactant. The liquid crystal domain is limited to a hexagonal phase, which is also very stable in temperature. Between these two phases, a wide biphasic domain is observed.

In this system, the micellar domain was investigated by SANS to determinate the aggregate structure. The investigated range of concentration was varied from 5 to 25 wt % of surfactant, and the temperature was fixed at 21 °C.

A set of the spectra obtained for three different surfactant concentrations (5, 10, and 25 wt %) prepared with D_2O and H_2O as water solvent are shown in Figure 1. The intensities are normalized, and the curves obtained for 5 and 10% of surfactant have been shifted, respectively, by a factor of 2 and of 5, which corresponds to the ratio between the disperse volume fractions of each sample and that of the sample containing 25% of surfactant. It can be observed that the intensities are proportional to the dispersed volume fraction since for all q larger than 0.09 $Å^{-1}$, the three curves are superimposed. However, a peak at smaller q values, around 0.075 $Å^{-1}$, characteristic of interparticular effects, becomes more and more pronounced with the increase of the surfactant concentration.

In addition, two peculiar water (H_2O/D_2O) contrasts near the extinction at zero angle have allowed to generate singularities in the experimental spectra. With 40% of D_2O, the presence of a large peak centered at 0.1 $Å^{-1}$ for all surfactant concentrations is noticed (Figure 2). This maximum is not due to interparticular effects because it already exists at 5% of surfactant but reflects the shape and the internal structure of the micellar aggregates. When the water contains 32% of D_2O, the curves present also a maximum that is weakly visible at low surfactant concentration and becomes more pronounced at 25% of surfactant. A satisfactory interpretation of the neutron scattering spectra can be performed by finding for the four contrasts the molecular model that would scatter, in q range 0.015−0.18 $Å^{-1}$, the neutron beam in the same way as the micelles. For the three surfactant concentrations, theoretical and experimental data are shown in Figure 2. The dots represent the experimental data, and the full lines correspond to the results obtained for the best model taking into account the interparticle interactions by the equivalent hard sticky sphere formalism at which a contribution associated to very short-range attractive forces considering a thin well with a width of 2 Å is added.

For 5% of $R_8^F(EO)_9$, the hard volume fraction corresponds to the disperse volume fraction, whereas for 10% and 25%, the hard volume fraction is, respectively, increased to 10% and 15%.

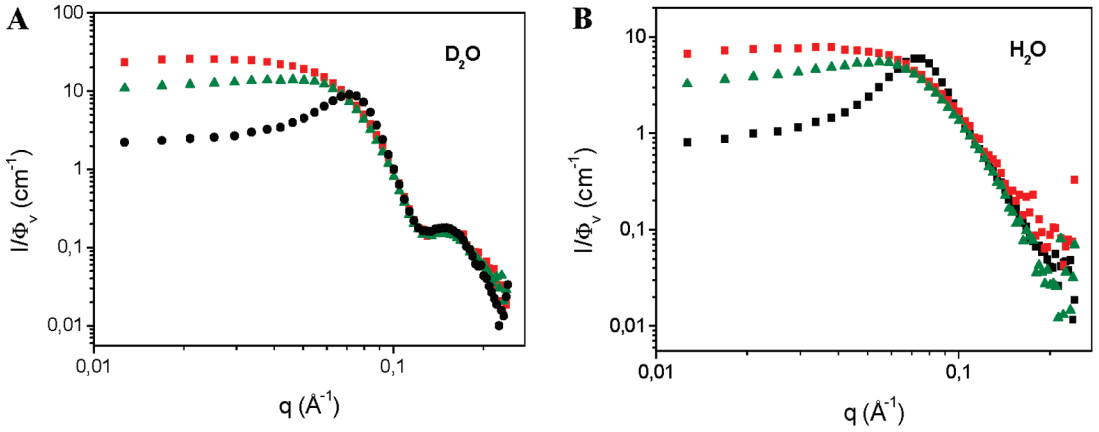

Figure 1. Normalized experimental SANS spectra $I = f(q)$ at 21 °C drawn in the double log representation for the samples with various surfactant concentrations: red square, 5%; green triangle, 10%; and black circle, 25%, of $R_8^F(EO)_9$ in D_2O (A) and H_2O (B).

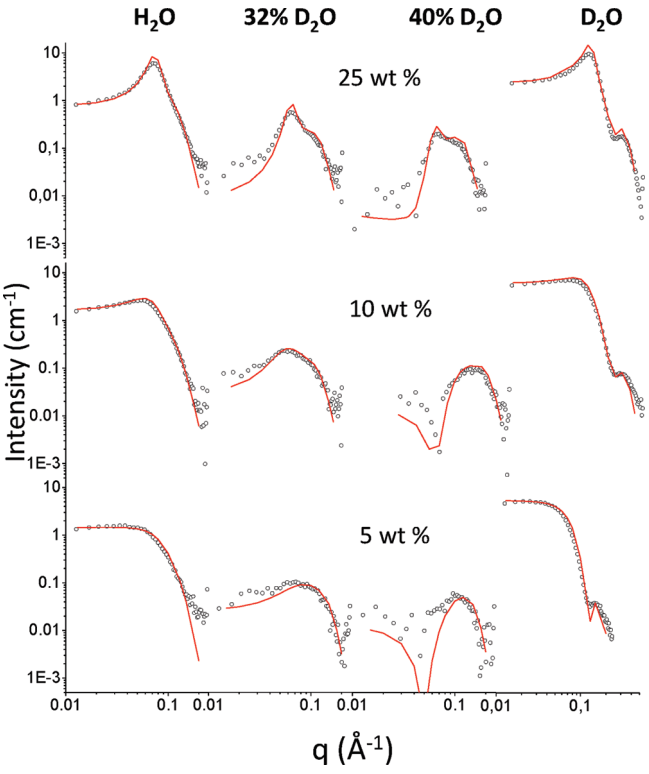

Figure 2. Comparison of the experimental results (○) with the theoretical $I(q)$ (full lines) curves for spheroidal shape of the aggregates for the $R_8^F(EO)_9$/water system at 21 °C for various surfactant concentrations and four water components, from left to right: pure H_2O, 32 and 40% D_2O, and pure D_2O.

Concerning the depth of the attractive well, it is lower than 0.5 kT for the most concentrated sample. The structure factor calculated with these parameters accounts for the scattered intensities of any concentrations. However, we notice that at the smallest q values for the 32 and 40% D_2O isotopic compositions, the curve fitting is not adapted. The interaction model used is not sensitive enough to the intensity levels of order 10^{-3} to 10^{-2} Å^{-1}, but all the experimental and theoretical curves fit well for q values higher than 0.07 Å^{-1}.

The results prove that in the investigated domain of compositions, the structures are not significantly affected by the variation of the surfactant concentration. In all cases, the micelles can be described by a set of slightly prolate particles with an axial ratio, which increases from 1.5 to 2.3 when the surfactant concentration is changed from 5 to 25 wt.%.

The aggregation number varies in the same way; its value is about 110 for 5%, 140 for 10%, and 170 for 25% of $R_8^F(EO)_9$. Consequently, the micellar size increases with the surfactant concentration, the highest dimension changes from 8.7 to 12.1 nm. Theses values are in agreement with those obtained from DLS experiments; indeed, for a diluted sample, the hydrodynamic diameter, obtained by this technique, is 9 nm. Concerning the fluorinated core, the smallest dimension remains constant and equal to 3.9 nm with the variation of the surfactant concentration. Therefore, with that kind of structure, the surfactant molecule is characterized by an extended conformation of the hydrophobic chains and a folded conformation of the oxyethylene oxide. As a result, the area per polar head is typically in the range from 0.55 to 0.59 nm^2, while the hydration rate (number of H_2O molecules inside the surfactant film per amphiphile molecule) is about 30. All of the parameters are given in Table 2.

$C_7F_{15}C_2H_4(OC_2H_4)_8OH$ [$R_7^F(EO)_8$] System in Water. Although the phase diagram was already reported elsewhere,[29] as we have used a new surfactant batch and since it is a commercial product, to obtain the exact phase boundaries, we need to establish the new phase diagram. Moreover, this system exhibits a lower consolute curve, which is particularly sensitive to the surfactant composition. With this surfactant batch, the cloud point is situated at 34 °C for 1% of surfactant. The micellar phase is stable at low temperature until 50% of surfactant, and the liquid crystal domain is composed only of the lamellar phase, which melts at 60 °C (Supporting Information, S1).

The experimental SANS analysis has been performed for 5, 10, and 25% of surfactant in water and for four isotopic compositions of water: pure H_2O, pure D_2O, and 32% and 48% of D_2O. The two last values correspond to compositions near the extinction at zero angle, which has been calculated at 36.4% of D_2O (see Table 1). The experimental spectra are reported in Figure 3 for two isotopic compositions of water. The intensities are normalized, and the curves obtained for 5 and 10% of surfactant have been shifted, respectively, by a factor of 2 and 5, which correspond to the ratio between the disperse volume fractions of each sample and that of the sample containing 25% of surfactant. From Figure 3, we can see that the scattered intensities are

dx.doi.org/10.1021/jp209853r |J. Phys. Chem. B 2012, 116, 261–268

Table 2. Morphological Parameters of $R_8^F(EO)_9$ Micellar Aggregates in Water[a]

$R_8^F(EO)_9$ (% w/w)	N	p	dimensions (nm)	hydrophilic chain thickness (nm)	hydrophobic chain thickness (nm)	σ (nm^2)	α (molar)
5	110	1.5	6.6/9	1.4	1.9	0.59	30
10	140	1.9	6.6/11	1.6	1.9	0.57	30
25	170	2.3	6.6/12	1.6	1.9	0.55	29

[a] N, aggregation number; p, ellipticity; σ, area per polar head; and α, number of water molecules per surfactant molecule in amphiphilic film.

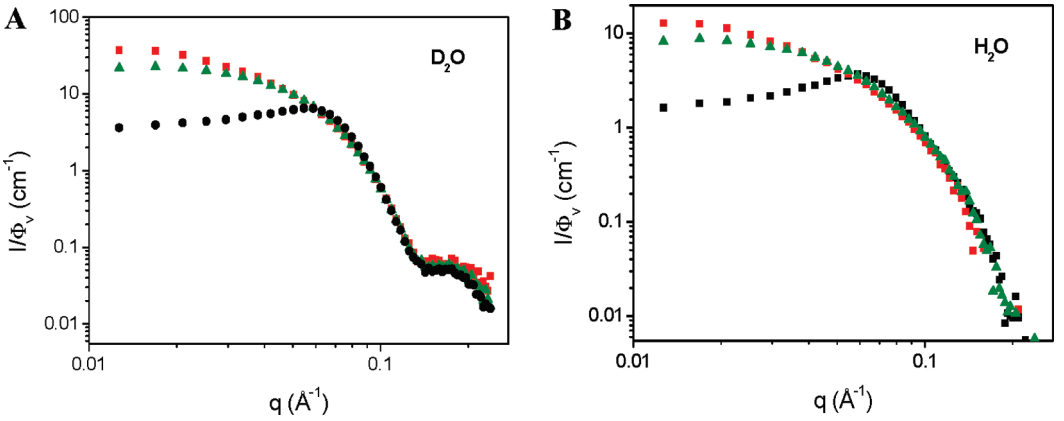

Figure 3. Normalized experimental SANS spectra $I = f(q)$ at 21 °C drawn in the double log representation for the samples having a $R_7^F(EO)_8$-concentration equal to red square 5%, green triangle 10%, and black circle 25% in D_2O (A) and H_2O (B).

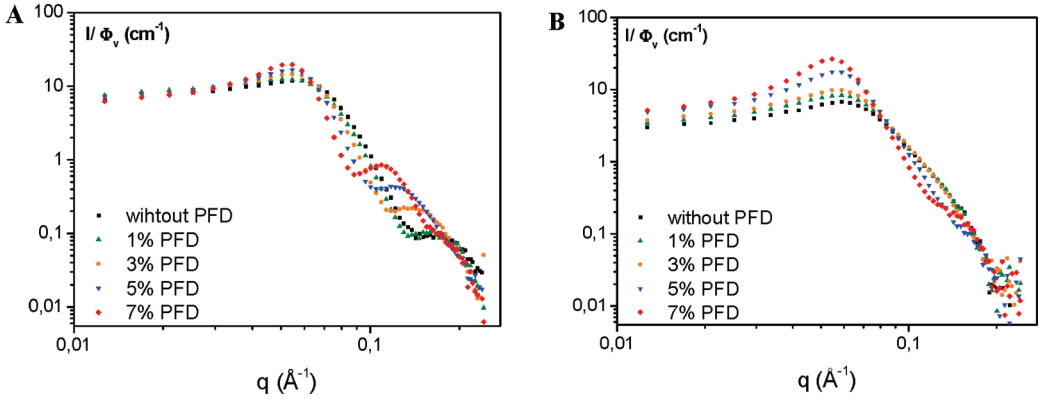

Figure 4. SANS spectra: effect of solubilization of perfluorodecalin in micelles of $R_7^F(EO)_8$ for 2 contrasts: (A) D_2O and (B) H_2O.

proportional to the dispersed volume fraction. Whatever the solvent, we can also observe on the spectrum of the sample having 25% of $R_7^F(EO)_8$ a significant peak located at 0.06 Å^{-1}, which is attributed to the interparticule interactions.

In this case, no particle model leads to a correct fitting of the experimental data, knowing that a same set of parameters should fit the experimental curves recorded for the various contrasts at a given surfactant concentration. The experiments carried out by DLS lead us to conclude that the aggregates are not spherical because the particles' average diameter, about 40 nm, does not correspond to the maximum length of the surfactant molecule, which is evaluated to be 4.1 nm. However, neither the prolate particles nor the rod-like models allow us to describe the experimental spectra.

Incorporation of Oil in the $R_7^F(EO)_8$ System. Contrary to $R_8^F(EO)_9$ micelles,[30] the $R_7^F(EO)_8$[29] ones can incorporate fluorinated oil, such as perfluorodecalin, at room temperature. The maximum quantity of perfluorodecalin that can be solubilized in the $R_7^F(EO)_8$ micelles is 7%. This value is determined for a water/surfactant ratio (R) of 3 (w/w). Therefore, we have studied the effect of the progressive incorporation of perfluorodecalin in the $R_7^F(EO)_8$ micelles on the aggregates structure. The experiments have been performed for $R = 3$ (w/w) with 1, 3, 5, and 7% of perfluorodecalin. At least 2 contrasts have been used. The recorded spectra with D_2O and H_2O as the water component are depicted in Figure 4. Upon the progressive addition of perfluorodecalin for both contrasts a peak around 0.06 Å^{-1} attributed to the interparticle effects, appears.

The intensity of this peak increases with the rise of the perfluorodecalin concentration. After systematic calculations with various models, we have obtained a series of results that appear coherent from a quantitative point of view. Indeed, if the concentration of perfluorodecalin is low, the best fits are obtained with anisotropic particles (prolate particles), which have

dx.doi.org/10.1021/jp209853r |J. Phys. Chem. B 2012, 116, 261–268

an ellipticity p = 4 (Figure 5). The more perfluorodecalin is added, the more the shape of the globules becomes spherical (p is less than 2 if the perfluorodecalin content is 7%). In the meantime, when the perfluorodecalin concentration increases from 1 to 7%, the aggregation number gradually rises from 300 to 430, whereas the surface per polar head slightly decreases from 0.54 to 0.49 nm^2. Hence, a full description of the interfacial film can be given. The conformation of the fluorocarbon chains is extended, and the penetration rate of the perfluorodecalin molecules inside these chains increases from 0 to 0.16 molecules per surfactant molecule with the quantity of the solubilized oil. Concerning the hydrophilic part, the chains are progressively coiled involving a change of the hydration degree (α) from 34 to 18. This corresponds to a variation from 4 to 1 of the water molecules per EO group into the surfactant film. The morphological parameters are summarized in Table 3.

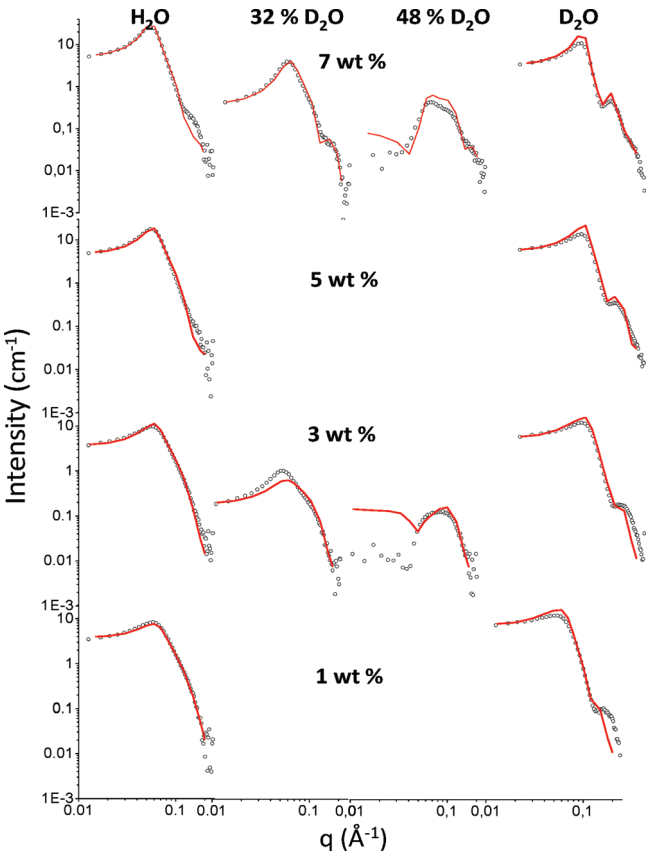

Figure 5. Comparison of the experimental (○) and the theoretical results (full lines) for spheroidal shape of the aggregate for the system $R_7^F(EO)_8$/water (water/surfactant = 3) at 21 °C for various contents of perfluorodecalin from bottom to top: 1, 3, 5, and 7% of oil and various contrasts from left to right: pure D_2O, 32 and 48% of D_2O, and pure H_2O.

DISCUSSION

The investigation of the $R_8^F(EO)_9$ and $R_7^F(EO)_8$ micellar solutions in water by SANS evidence that both systems have different micelle morphology. As a matter of fact, for all the isotopic mixtures and up to 25 wt % of surfactant, a model of quasi-spherical globules describes the $R_8^F(EO)_9$ micelles in water in a satisfying way. Contrarily, the experimental curves of $R_7^F(EO)_8$ in water cannot be fitted considering a small particle model. For this system, several observations support the fact that the particles are elongated. First, the hydrodynamic radius, determined by QELS, is 40 nm. This value does not match with spherical particles as the surfactant chain length (hydrophilic + hydrophobic) is estimated to be 4.1 nm. Second, these micellar systems, which are isotropic at rest, exhibit a notable birefringent upon shaking as soon as the $R_7^F(EO)_8$ concentration reaches 5 wt % and becomes strong for R = 3, i.e, for 25 wt.% of surfactant. For this ratio, we have studied the effect of the perfluorodecalin incorporation on the micellar structure. Results obtained by SANS show a change in the shape of the objects, which become spheroid upon the addition of 1 wt % of perfluorodecalin. When the fluorocarbon concentration is maximal, the globules adopt a quasi-spherical shape. A few years ago, this kind of behavior was already reported for hydrogenated systems. Indeed, the study of the structural evolution of the molecular aggregates of C_mEO_n surfactants showed that the micelles became less anisometric with progressive oil incorporation, and the demixing occurred when the aggregates are spherical.[31] More recently, Aramaki et al. have also reported that the structures of the $C_8F_{17}SO_2(C_3H_7)N(C_2H_4O)_{10}$ aqueous solutions adopt a similar behavior, and for this system, worm like micelles[32] have been identified by SAXS. A complementary study shows that the addition of a small amount of perfluoropolyether oil induces a dramatic change in the structure of micelles. In fact, a transition from long cylindrical micelles to globular like particles[33] occurs when the oil is incorporated.

Using $R_8^F(EO)_9$ or $R_7^F(EO)_8$ micellar solutions, mesoporous silica materials have been prepared through the self-assembly mechanism (CTM). As the building blocks are the micelles, the CTM occurs at low surfactant concentrations. The synthesis conditions of the materials have been reported elsewhere.[24] Hexagonal molecular sieves have been prepared at 80 °C with $R_8^F(EO)_9$ micelles, on a wide range of the surfactant concentrations in aqueous solution (5−20 wt %). As a matter of fact, three reflections at q ratios 1:$\sqrt{3}$:2, consistent with a hexagonal symmetry, are observed on the SAXS pattern. According to the IUPAC classification, a type IV isotherm is obtained by nitrogen adsorption−desorption analysis. The obtained materials exhibit a high specific surface area and a narrow pore size distribution,

Table 3. Morphological Parameters of Perfluorodecalin Swollen Aggregates of $R_7^F(EO)_8$ in Water[a]

perfluorodecalin (% w/w)	N	p	dimensions (nm)	hydrophilic chain thickness (nm)	hydrophobic chain thickness (nm)	σ (nm^2)	α	β
1	300	4	8/20	1.8	1.5	0.54	34	0.01
3	320	3.5	8/19	1.7	1.6	0.53	31	0.07
5	370	2.6	8/17	1.5	1.7	0.52	21	0.14
7	430	1.9	9/15	1.5	1.8	0.49	18	0.16

[a] N, aggregation number; p, ellipticity; σ, area per polar head; and α and β stand for the number of water and perfluorodecalin molecules per surfactant molecule in the amphiphilic film, respectively.

dx.doi.org/10.1021/jp209853r |J. Phys. Chem. B 2012, 116, 261–268

which its maximum varies from 4.3 to 6.0 nm depending on the surfactant concentration. Beyond 20 wt % of surfactant, the loss of the mesopore ordering occurs and only one broad peak, characteristic of a wormhole-like structure analogue to MSU is observed on the SAXS patterns. By contrast, in the same synthesis condition of, i.e., pH, surfactant/silica molar ratio, hydrothermal temperature, and duration, only wormhole-like structures are recovered with $R_7^F(EO)_8$.[25] For the latter system, the mesopore ordering occurs when the materials are prepared from swollen micelles.[29] The addition of perfluorodecalin up to 7 wt % involves a swelling of the mesopores from 5 to 6.8 nm in relation with the increase of the micelles sizes evidenced by SANS in the study reported here. The overall results obtained for both the $R_8^F(EO)_9$ and the $R_7^F(EO)_8$ systems seem to indicate that the presence of spheroid micelles favors the mesopore ordering when materials are synthesized through the self-assembly mechanism. Considering various hydrogenated and fluorinated surfactant based systems, we have shown that several conditions have to be fulfilled to obtain a hexagonal mesopore ordering. First, the ratio between the volume of the hydrophilic part of the surfactant and the volume of its hydrophobic part (V_A/V_B) should be between 0.95 and 1.78.[22] However, this condition is not sufficient. Indeed, the presence of a cloud point curve disturbs the self-assembly mechanism, and to prepare ordered mesoporous materials, the temperature at which the silica precursor is added to the micellar solution should not be close to the phase separation temperature.[17] The V_A/V_B ratios for the $R_8^F(EO)_9$ and the $R_7^F(EO)_8$ surfactant are 1.89 and 1.28, respectively. Thus, both systems should lead to the formation of an ordered structure. However, while micellar solutions of $R_8^F(EO)_9$ involve the formation of a hexagonal mesopore channel array, only disordered structures are recovered when the synthesis is performed from $R_7^F(EO)_8$ micellar solutions that exhibit a cloud point at 34 °C. Therefore, one can think that the pore ordering of the mesoporous silica is related to the shape of the micelles and, in particular, that the presence of spherical micelles favors the mesopore ordering. We can notice here that the presence of elongated micelles at room temperature for the $R_7^F(EO)_8$ based system is not likely correlated to the existence of the critical point at higher temperature, even if it is well-known that at a temperature very close to the critical point (1 to 2 °C), critical fluctuations appear,[20,34] leading to the formation of large micelles. In our case, the fluorinated micelle structure has been investigated at a temperature 14 °C below the critical point. In addition, some systems present a cloud point closer to the one of the $R_7^F(EO)_8$ surfactant, and depending on the molecular structure of the surfactant, the micelles in water adopt either an elongated $[C_{12}(EO_6)]$[35] or a spherical $[C_{12}(EO)_8]$[36] shape.

In the literature, only few studies are focused on the relationship between the nonionic surfactant micelle structures and the formation of ordered mesoporous materials. The triblock copolymer P123 supports this hypothesis. Indeed, it is well admitted that this surfactant forms spherical micelles, and the materials prepared from the P123 micellar solution have a hexagonal channel array.[8,9] However, the $C_8F_{17}SO_2(C_3H_7)N(C_2H_4O)_{10}$ system, which presents a cloud point at around 50 °C, contradicts this rule. As indicated below, it has been reported that this surfactant gives rise to elongated micelles. Starting from these wormhole-like micelles, Esquena et al. have prepared hexagonal mesoporous materials.[37] Nevertheless, it should be noted that the synthesis conditions are astonishing as the silica precursor is added under a very acidic pH value and at a temperature situated above the cloud point. This means that the system is biphasic and that the materials are not synthesized through the self-assembly mechanism. The synthesis conditions are, therefore, very different from the ones reported in our studies, so we can assume that spherical micelles are required to obtain the hexagonal mesopore ordering.

CONCLUSIONS

The structure of nonionic fluorinated micelles has been investigated by SANS and correlated to the pore ordering of mesoporous silica materials prepared through the cooperative templating mechanism (CTM). Two surfactants belonging to the polyoxyethylene fluoroalkyl ether family have been considered. The main difference between the two surfactants is the number of oxyethylene groups and the number of carbon of the fluoroalkyl chain. The micelles of the more hydrophilic surfactant $[R_8^F(EO)_9]$ are stable with temperature, and the analysis of the neutron scattering data allows us to analyze the evolution of the micelle structure at 20 °C as a function of the surfactant concentration. The globules can be described by prolate spheroids, with the axial ratio increasing from 1.5 to 2.3 when the surfactant concentration is changed from 5 to 25 wt %. The aggregation number varies in the same way from 110 to 170. Looking at the mesoporous silica materials, a hexagonal pore ordering can be obtained in the overall investigated range of surfactant concentration.

The second surfactant, $R_7^F(EO)_8$ also forms micelles, and its less hydrophilic nature can be highlighted by the presence in the phase diagram of a lower consolute curve. The critical temperature is situated at 34 °C. In that case, no small particles model allows an acceptable fitting of the SANS curves recorded at 20 °C. In addition, no ordered silica materials can be recovered; only wormhole-like structures can be obtained. However, the solubilization of fluorocarbon into the $R_7^F(EO)_8$ micelles leads to a mesopore ordering. The SANS study reveals that the progressive incorporation of the fluorocarbon in the core of the micelles involves a change of both size and shape of the micelles. As a matter of fact, a model of elongated spheroids, with axial ratio decreasing from 4 to 2 when the oil concentration is changed from 1 to 7 wt % can be used to fit the SANS curves.

Therefore, the study reported here evidence that from the mesoporous point of view, ordered mesostructures are favored whenever the size of the micelles is reduced.

ASSOCIATED CONTENT

Supporting Information. Phase diagram of $C_7F_{15}C_2H_4(OC_2H_4)_8OH$ $[R_7^F(EO)_8]$ in water. This material is available free of charge via the Internet at http://pubs.acs.org.

ACKNOWLEDGMENT

We thank DuPont de Nemours Belgium for providing the $R_8^F(EO)_9$ and $R_7^F(EO)_8$ used in this study. We would also like to thank Anna May for revising the English.

REFERENCES

(1) Beck, J. S.; Vartuli, J. C.; Roth, W. J.; Leonowicz, M. E.; Kresge, C. T.; Schmitt, K. D.; Chu, C. T. W.; Olson, D. H.; Sheppard, E. W.; McCullen, S. B.; Higgins, J. B.; Schlenker, J. L. *J. Am. Chem. Soc.* **1992**, *114*, 10834–10843.

(2) Wan, Y.; Zhao, D. *Chem. Rev.* **2007**, *107*, 2821–2860.
(3) Bagshaw, S. A.; Prouzet, E.; Pinnavaia, T. J. *Science* **1995**, *269*, 1242–1244.
(4) Zhao, D.; Huo, Q.; Feng, J.; Chmelka, B. F.; Stucky, G. D. *J. Am. Chem. Soc.* **1998**, *120*, 6024–6036.
(5) Landry, C. C.; Tolbert, S. H.; Gallis, K. W.; Monnier, A.; Stucky, G. D.; Norby, P.; Hanson, J. C. *Chem. Mater.* **2001**, *13*, 1600–1608.
(6) Glinka, C. J.; Nicol, J. M.; Stucky, G. D.; Ramli, E.; Margolese, D.; Huo, Q.; Higgins, J. B.; Leonowicz, M. E. *J. Porous Mater.* **1996**, *3*, 93–98.
(7) Linton, P.; Rennie, A. R.; Zackrisson, M.; Alfredsson, V. *Langmuir* **2009**, *25*, 4685–4691.
(8) Khodakov, A. Y.; Zholobenko, V . L.; Impéror-Clerc, M.; Durand, D. *J. Phys. Chem. B* **2005**, *109*, 22780–22790.
(9) Sundblom, A.; Oliveira, C. L. P.; Palmqvist, A. E. C.; Pedersen, J. S. *J. Phys. Chem. C* **2009**, *113*, 7706–7713.
(10) Impéror-Clerc, M.; Grillo, I.; Khodakov, A. Y.; Durand, D.; Zholobenko, V. L. *Chem. Commun.* **2007**, 834–836.
(11) Castelletto, V.; Hamley, I. W.; Pedersen, J. S. *J. Chem. Phys.* **2002**, *117*, 8124–8129.
(12) Flodström, K.; Wennerström, H.; Aldfredsson, V. *Langmuir* **2004**, *20*, 680–688.
(13) Ruthstein, S.; Schmidt, J.; Kesselman, E.; Talmon, Y.; Goldfarb, D. *J. Am. Chem. Soc.* **2006**, *128*, 33663374.
(14) Patarin, J.; Lebeau, B.; Zana, R. *Curr. Opin. Colloid Interface Sci.* **2002**, *7*, 107–115.
(15) Zholobenko, V.; Khodakov, A. Y.; Impéror-Clerc, M.; Durand, D.; Grillo, I. *Adv. Colloid Interface Sci.* **2008**, *142*, 67–74.
(16) Sundblom, A.; Oliveira, C. L. P.; Pedersen, J. S.; Palmqvist, A. E. C. *J. Phys. Chem. C* **2010**, *114*, 34833492.
(17) Michaux, F.; Blin, J. L.; Stébé, M. J. *Langmuir* **2008**, *24*, 1044–1052.
(18) Ravey, J. C. *J. Colloid Interface Sci.* **1983**, *94*, 289–291.
(19) El Moujahid, C.; Ravey, J. C.; Schmitt, V.; Stébé, M. J. *Colloids Surf., A* **1998**, *136*, 289–297.
(20) Triolo, R.; Magid, L. J.; Johnson, J. S.; Child, H. R. *J. Phys. Chem.* **1982**, *86*, 3689–3695.
(21) Kim, J. M.; Sakamoto, Y.; Hwang, Y. K.; Kwon, Y.-U.; Terasaki, O.; Park, S.-E.; Stucky, G. D. *J. Phys. Chem. B* **2002**, *106*, 2552–2558.
(22) Michaux, F.; Blin, J. L.; Stébé, M. J. *J. Phys. Chem. B* **2008**, *112*, 11950–11959.
(23) Ravey, J. C.; Stébé, M. J. *Colloids Surf., A* **1994**, *84*, 11–31.
(24) Blin, J. L.; Lesieur, P.; Stébé, M. J. *Langmuir* **2004**, *20*, 491–498.
(25) Blin, J. L.; Bleta, R.; Stébé, M. J. *J. Colloid Interface Sci.* **2006**, *300*, 765–773.
(26) Ravey, J. C.; Stébé, M. J.; Sauvage, S. *Colloids Surf., A* **1994**, *91*, 237–257.
(27) Ravey, J. C.; Buzier, M.; Picot, C. *J. Colloid Interface Sci.* **1984**, *97*, 9–25.
(28) Ravey, J. C.; Buzier, M. In *Surfactants in Solution*; Mittal, K. L., Lindman, B., Eds.; Plenum Press: New York, 1984; Vol. 3, pp 1759−1779.
(29) Bleta, R.; Blin, J. L.; Stébé, M. J. *J. Phys. Chem. B* **2006**, *110*, 23547–23556.
(30) Blin, J. C.; Stébé, M. J. *J. Phys. Chem. B* **2004**, *108*, 11399–11405.
(31) Ravey, J. C.; Buzier, M. In *Surfactants in Solution*; Mittal, K. L. Ed.; Plenum Press: New York, 1989; Vol. 8, pp 117−132.
(32) Shrestha, L. K.; Sharma, S. C.; Sato, T.; Glatter, O.; Aramaki, K. *J. Colloid Interface Sci.* **2007**, *316*, 815–824.
(33) Sharma, S. C; Shrestha, R. G.; Shrestha, L. K.; Aramaki, K. *J. Phys. Chem. B* **2009**, *113*, 1615–1622.
(34) Corti, M.; Degiorgio, V. *Phys. Rev. Lett.* **1980**, *45*, 1045–1048.
(35) Gapinski, J.; Szymanski, J.; Wilk, A.; Kohlbrecher, J.; Patkowski, A.; Holyst, R. *Langmuir* **2010**, *26*, 9304–9314.
(36) Imai, M.; Yoshida, I.; Iwaki, T.; Nakaya, K. *J. Chem. Phys.* **2005**, *122*, 44906.
(37) Esquena, J.; Rodriguez, C.; Solans, C.; Kunieda, H. *Micropor. Mesopor. Mater.* **2006**, *92*, 212–219.